eLIFE
elifesciences.org

Figures and figure supplements

Global analysis of p53-regulated transcription identifies its direct targets and unexpected regulatory mechanisms

Mary Ann Allen, et al.

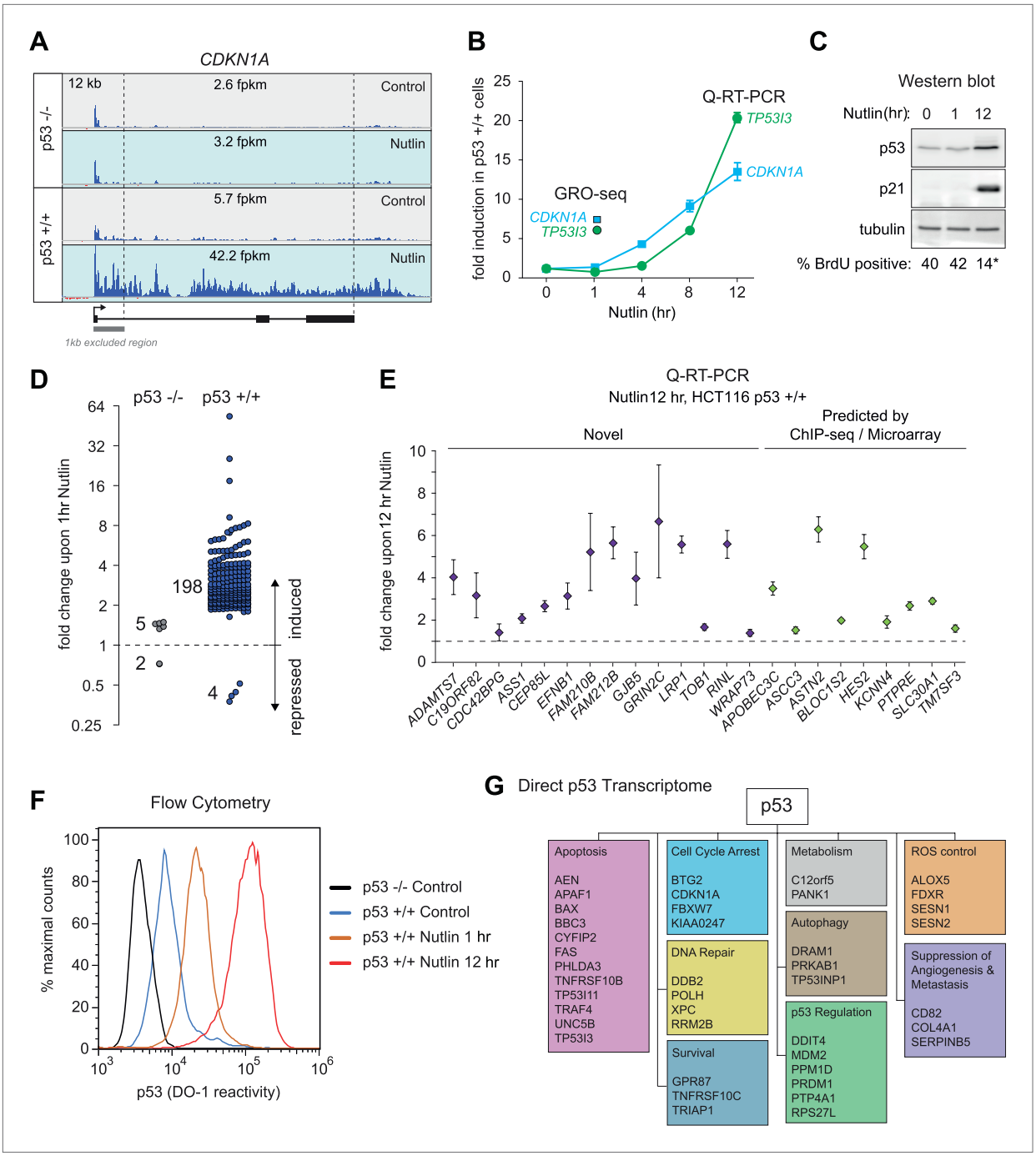

Figure 1. GRO-seq analysis of the p53 transcriptional program. (**A**) GRO-seq results for the p53 target locus *CDKN1A* (*p21*). Isogenic p53 −/− and p53 +/+ HCT116 cells were treated for 1 hr with either 10 μM Nutlin-3a (Nutlin) or vehicle (DMSO, Control). Fragments per kilobase per million reads (fpkm) are shown for the intragenic region. The first kilobase downstream of the transcription start site (TSS) was excluded from the fpkm calculation to minimize effects of RNAPII pausing. The total genomic region displayed is indicated in the top left corner. Blue signals are reads mapping to the sense strand, red signals are reads mapping to the antisense strand. See ***Figure 1—figure supplement 1A*** for results of the *TP53I3* locus. (**B**) GRO-seq detects transactivation of the canonical p53 target genes *CDKN1A* and *TP53I3* at 1 hr of Nutlin treatment, prior to any detectable increase in steady state mRNA levels as measured by Q-RT-PCR. (**C**) A 1 hr time point of Nutlin treatment does not produce significant p53 accumulation, p21 protein induction or a decrease in number of S phase cells as measured by BrdU incorporation assays. * indicates $p<0.05$. See also ***Figure 1—figure supplement 1B*** for quantification data of BrdU assays. (**D**) Genome-wide analysis using the DESeq algorithm identifies 198 annotated gene loci transactivated upon Nutlin treatment only in HCT116 p53 +/+ cells. See ***Supplementary file 1*** for a detailed annotation of these genes. (**E**) Q-RT-PCR validates induction of novel and predicted direct p53 target genes upon 12 hr of Nutlin treatment. mRNA expression

Figure 1. Continued on next page

Figure 1. Continued

was normalized to 18s rRNA values and expressed as fold change Nutlin/DMSO. Data shown are the average of three biological replicates with standard errors from the mean. (**F**) Flow cytometry analysis using the DO-1 antibody recognizing the MDM2-binding surface in the p53 transactivation domain 1 (TAD1) reveals increased reactivity as early as 1 hr of Nutlin treatment, indicative of unmasking of the TAD1 at this early time point. (**G**) p53 directly activates a multifunctional transcriptional program at 1 hour of Nutlin treatment, including many canonical apoptotic genes. See ***Supplementary file 1*** for a complete list and annotation.

DOI: 10.7554/eLife.02200.003

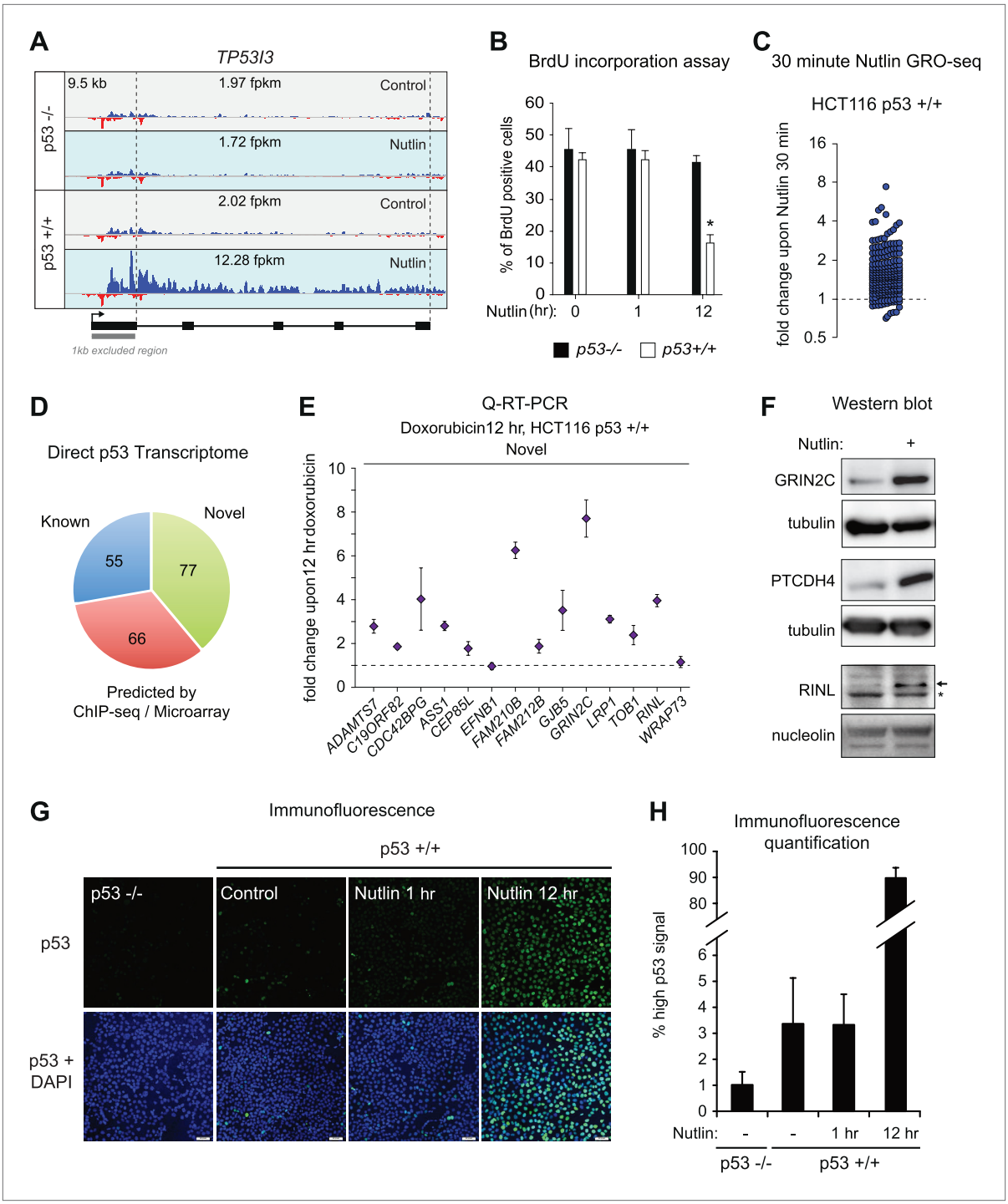

Figure 1—figure supplement 1. GRO-seq reveals the immediate direct p53 transcriptional response.

DOI: 10.7554/eLife.02200.004

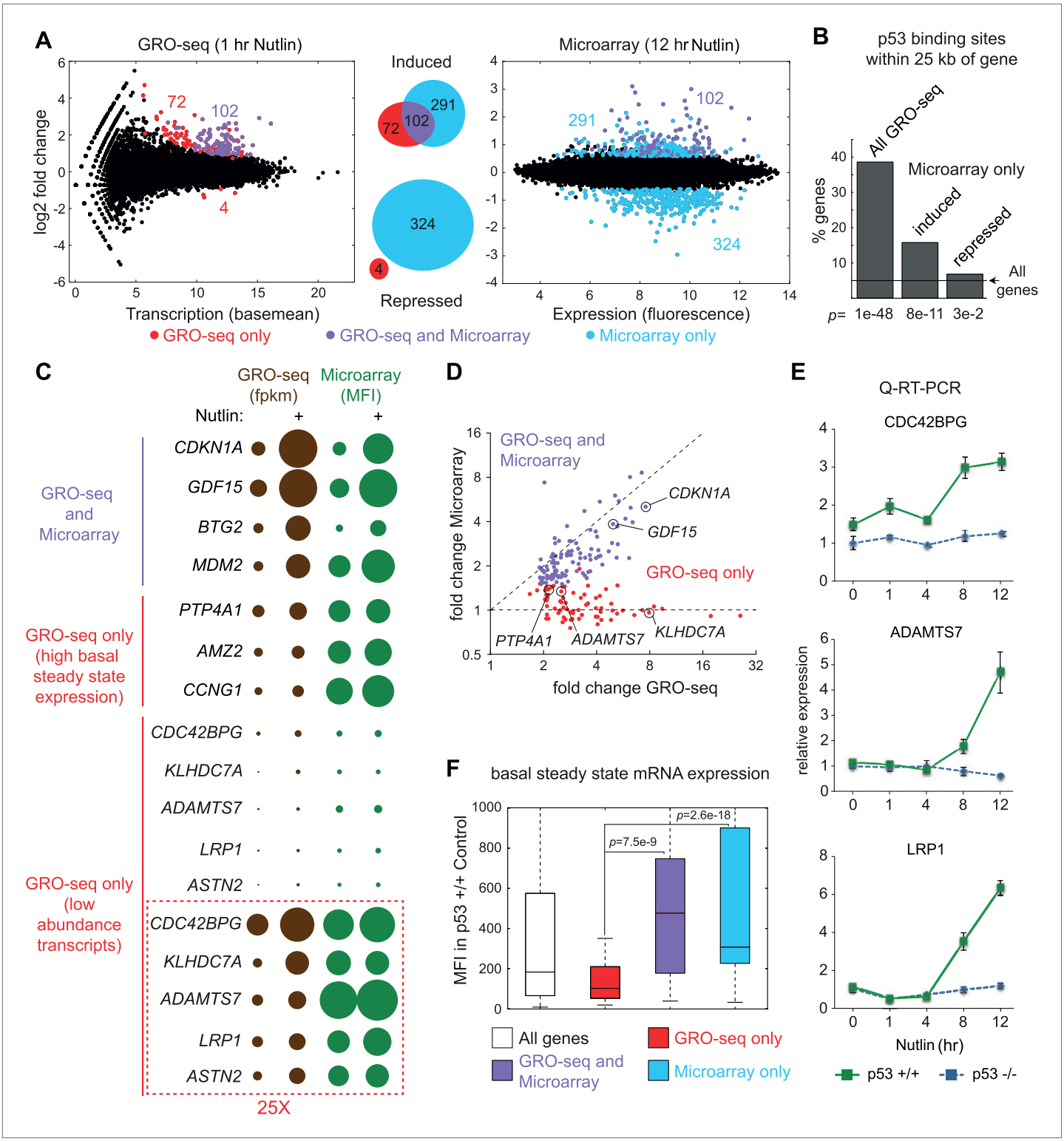

Figure 2. Global analysis of p53 effects on RNA synthesis vs steady state levels. (**A**) MAplots for GRO-seq and microarray gene profiling experiments in HCT116 p53 +/+ cells after 1 hr and 12 hr of Nutlin treatment, respectively. Colors indicate whether genes scored as statistically different in both platforms (purple), in the GRO-seq only (red) or the microarray experiment only (blue). (**B**) Few genes downregulated in the microarray experiment show p53 binding within 25 kb of the gene, suggestive of indirect regulation. (**C**) Bubble plots displaying relative signals derived from the GRO-seq and microarray experiments illustrate how genes with very high basal expression or very low transcription are not significantly affected at the steady state level as measured by microarray. For the *CDC42BPG*, *KLHDC7A*, *ADAMTS7*, *LRP1* and *ASTN2* loci,

Figure 2. Continued on next page

Figure 2. Continued

the signals were replotted at 25-fold magnification. (**D**) Scatter plot showing comparative fold induction for p53 target genes transactivated at 1 hr Nutlin treatment between the GRO-seq and microarray experiments. (**E**) Q-RT-PCR indicates that many low abundance transcripts upregulated by GRO-seq are indeed induced at the steady state level. (**F**) Box and whisker plots showing the expression of various gene sets as detected by microarray.

DOI: 10.7554/eLife.02200.005

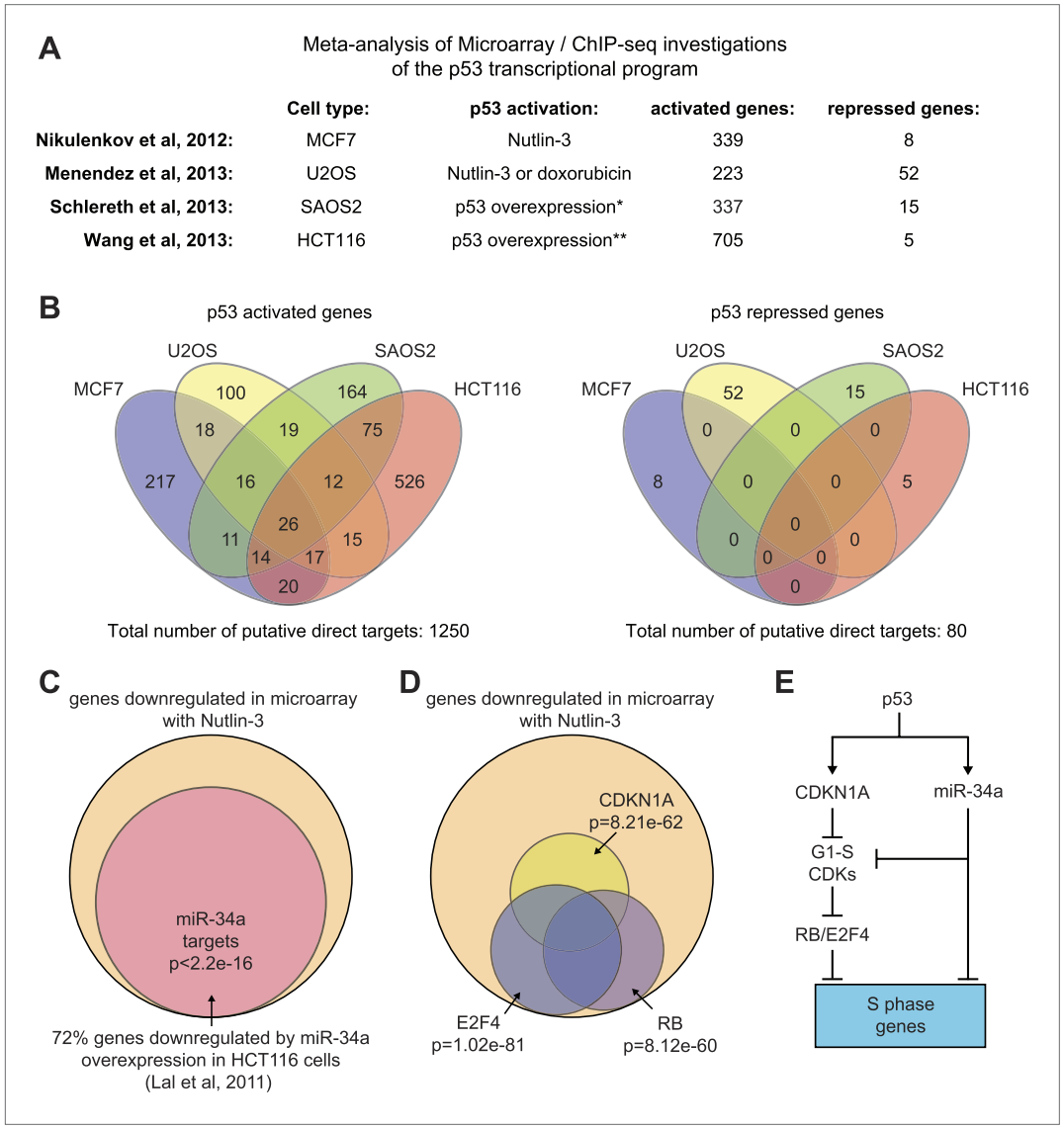

Figure 2—figure supplement 1. Mechanisms of indirect gene repression by p53.

DOI: 10.7554/eLife.02200.006

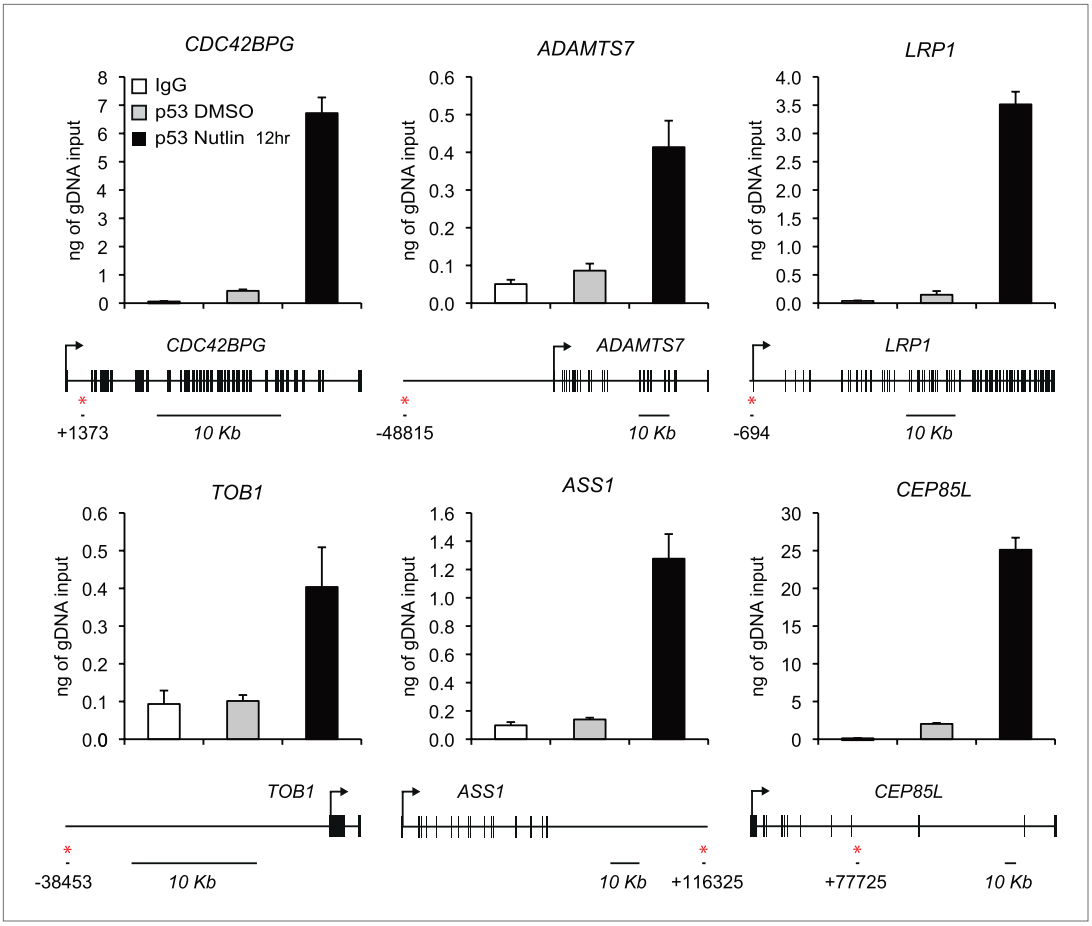

Figure 2—figure supplement 2. ChIP analysis of novel p53 target genes.
DOI: 10.7554/eLife.02200.007

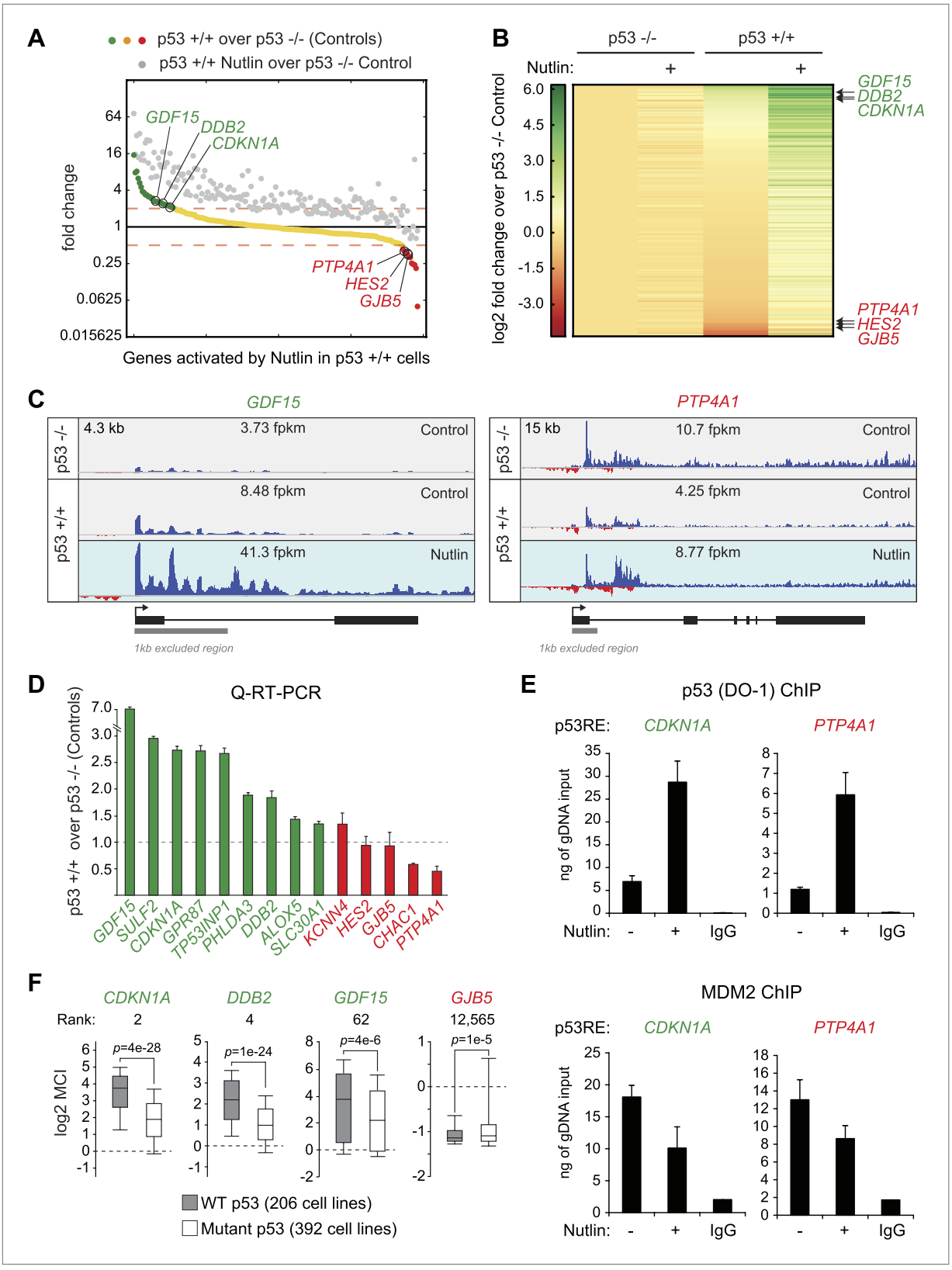

Figure 3. p53 exerts varying activating and repressing effects on its target genes prior to MDM2 inhibition. (**A**) 198 genes activated upon 1 hr Nutlin treatment in HCT116 p53 +/+ cells are ranked from left to right based on their basal transcription in p53 +/+ cells over p53 −/− cells. Green indicates genes whose basal transcription is greater than twofold in p53 +/+ cells, red indicates lesser than twofold. Grey dots display the transcription of the

Figure 3. Continued on next page

Figure 3. Continued

same genes in Nutlin-treated p53 +/+ cells. (**B**) Heatmap displaying relative transcriptional activity of direct p53 target genes identified by GRO-seq relative to control p53 −/− cells. Genes are sorted based on their transcription in control p53 +/+ cells. (**C**) Genome browser views of representative genes whose basal transcription is higher (*GDF15*) or lower (*PTP4A1*) in the presence of MDM2-bound p53. See ***Figure 3—figure supplement 1A*** for matching RNAPII ChIP data. (**D**) Q-RT-PCR measurements of genes whose basal transcription was found to be 2x higher (green) or lower (red) in the presence of MDM2-bound p53. (**E**) ChIP assays show binding of p53 and MDM2 to the p53REs in the *CDKN1A* and *PTP4A1* gene loci (−2283 bp and +1789 relative to TSS, respectively), prior to inhibition of the p53-MDM2 interaction by Nutlin. Nutlin treatment leads to increased p53 signals with the DO-1 antibody recognizing the p53 TAD1, concurrently with a decrease in MDM2 signals. MDM2 ChIP was performed in SJSA cells carrying a MDM2 gene amplification **F**. Oncomine gene expression analysis of 598 cancer cell lines of varied p53 status shows that *CDKN1A*, *DDB2* and *GDF15* are more highly expressed in wild type p53 cell lines, whereas *GJB5* is more highly expressed in mutant p53 cell lines. The ranking position of these genes is also indicated.

DOI: 10.7554/eLife.02200.008

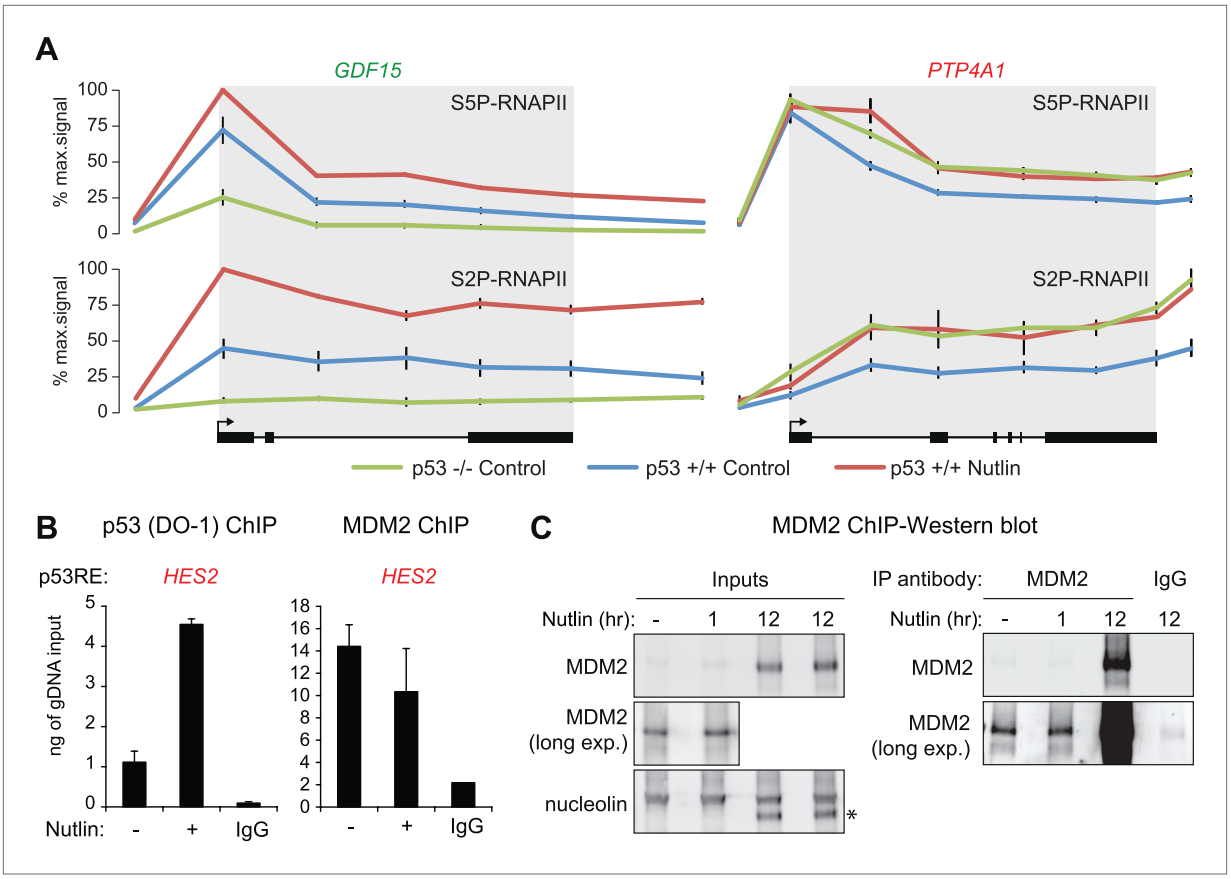

Figure 3—figure supplement 1. Differential effects of p53 on the basal transcription of its target genes.

DOI: 10.7554/eLife.02200.009

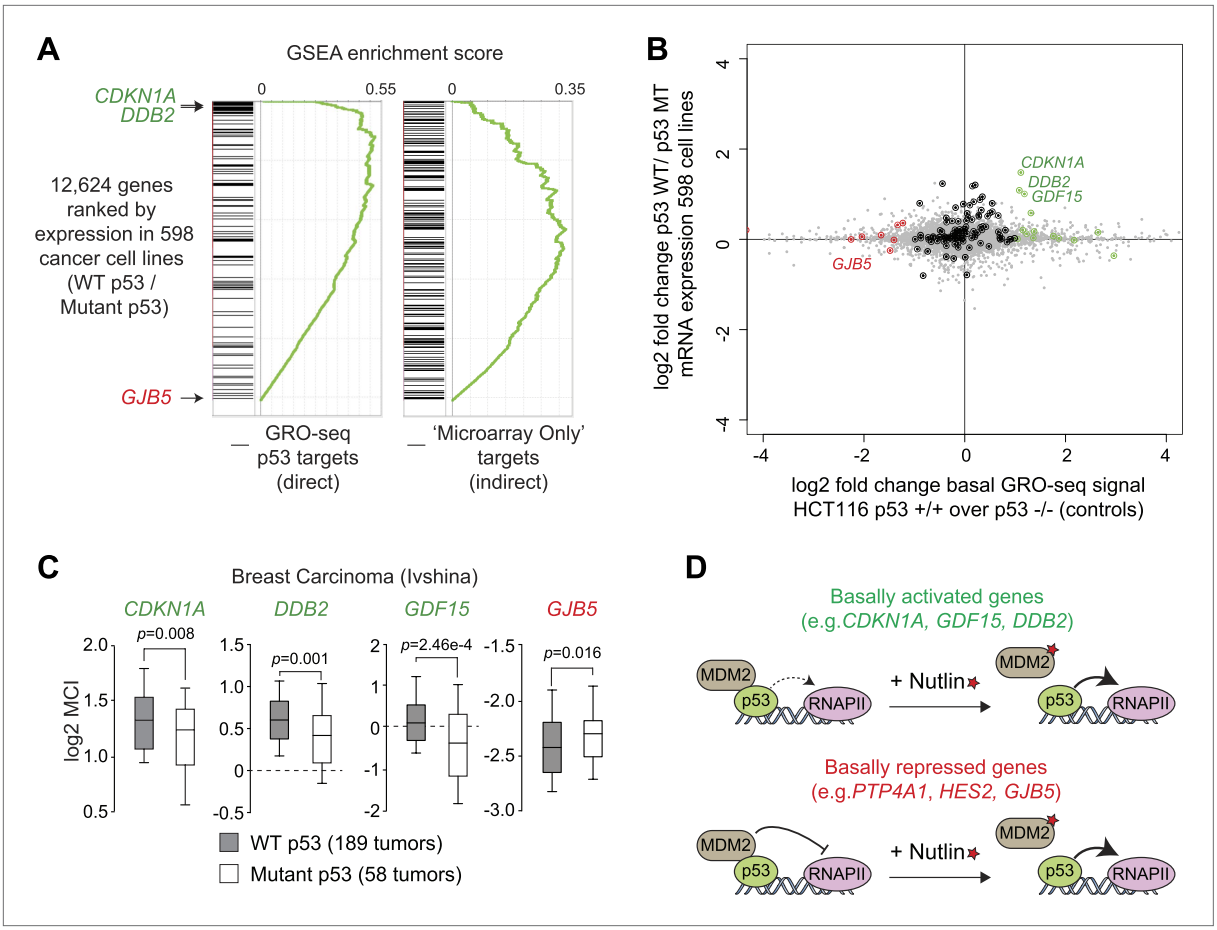

Figure 3—figure supplement 2. p53 mutational status affects the basal expression of its target genes.
DOI: 10.7554/eLife.02200.010

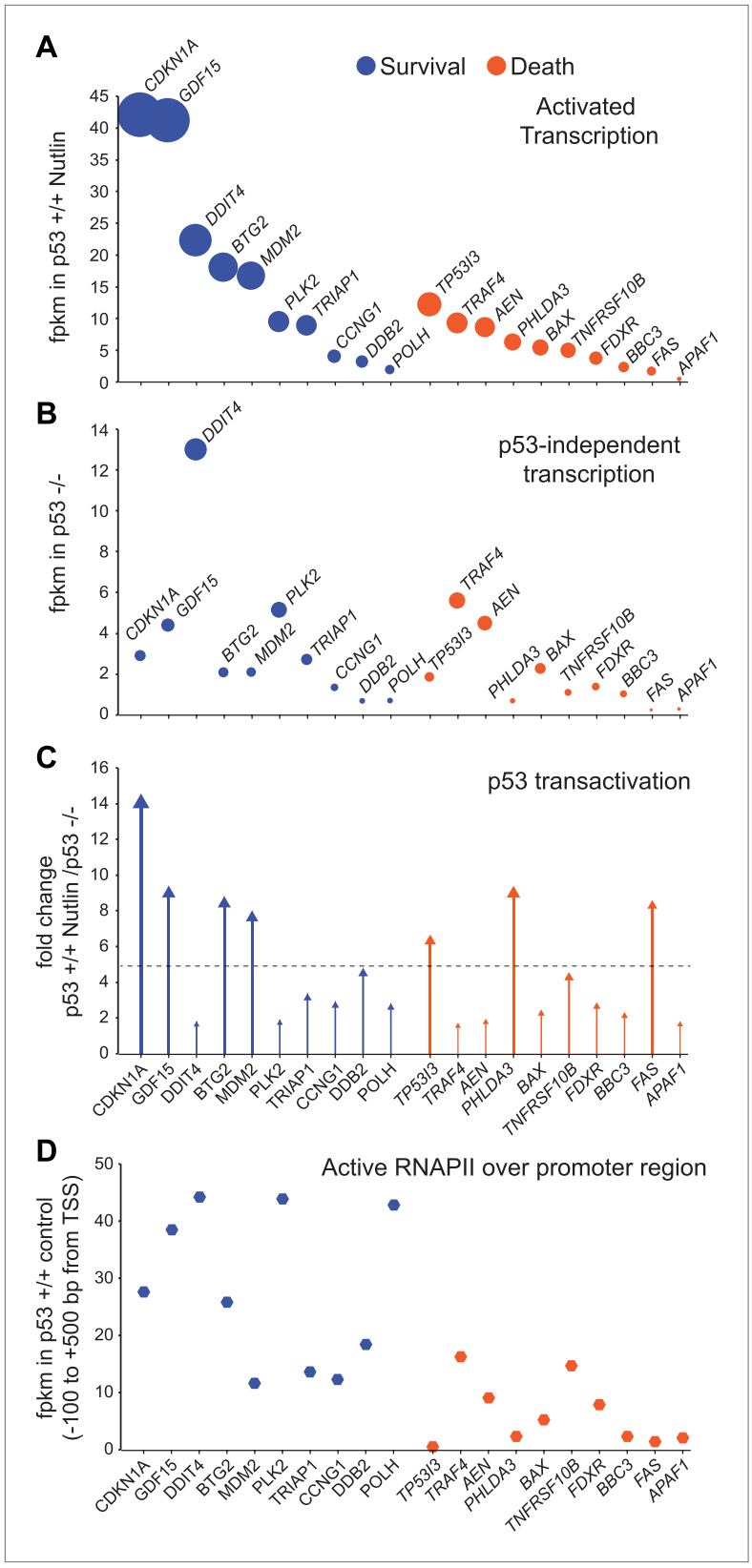

Figure 4. GRO-seq analysis of key survival and death genes within the p53 network. (**A**) The 10 most transcribed pro-survival and pro-apoptotic genes identified by GRO-seq ranked by decreasing transcriptional output in Nutlin-treated p53 +/+ cells. The surface of the bubbles represents the GRO-seq signal output relative to the

Figure 4. Continued on next page

Figure 4. Continued

CDKN1A locus. (**B**) Transcriptional output of same genes shown in **A** in p53 −/− cells. (**C**) Fold change analysis showing the overall effect of p53 on the transcription of its survival and apoptotic targets. (**D**) Survival genes within the p53 network tend to carry more proximally bound, transcriptionally engaged RNAPII over their promoter regions than apoptotic genes.

DOI: 10.7554/eLife.02200.011

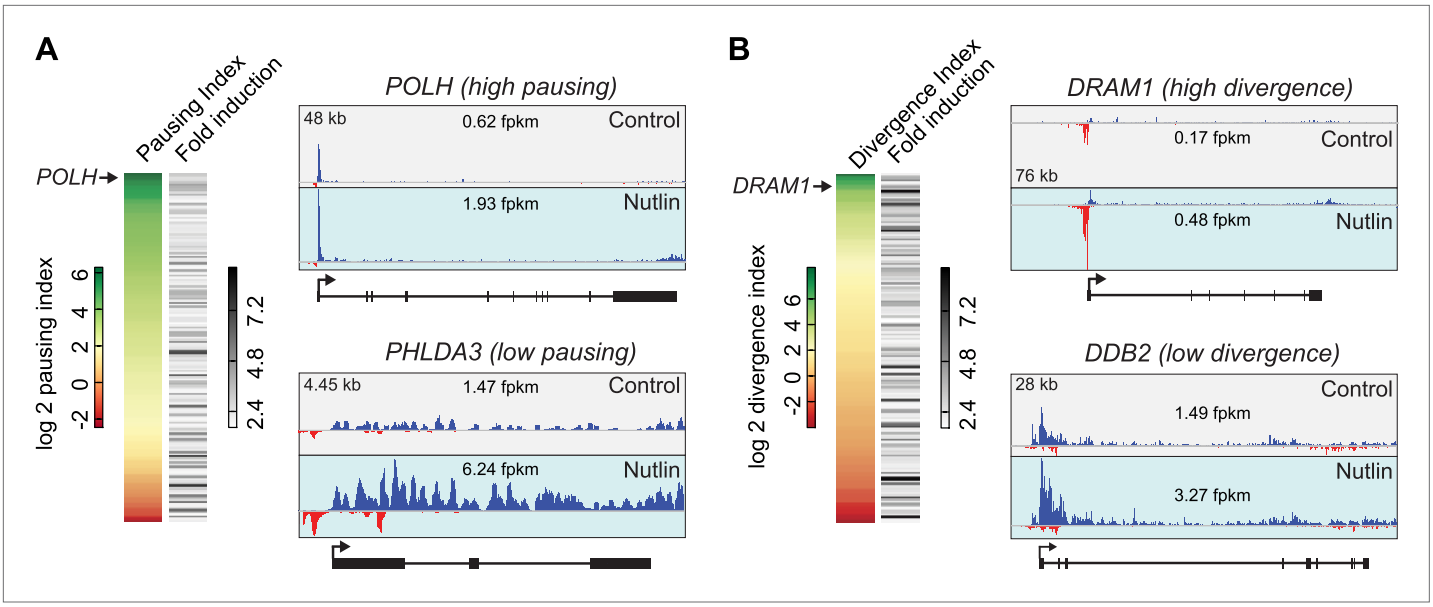

Figure 4—figure supplement 1. p53 target genes display a wide range of RNAPII pausing and promoter divergence.

DOI: 10.7554/eLife.02200.012

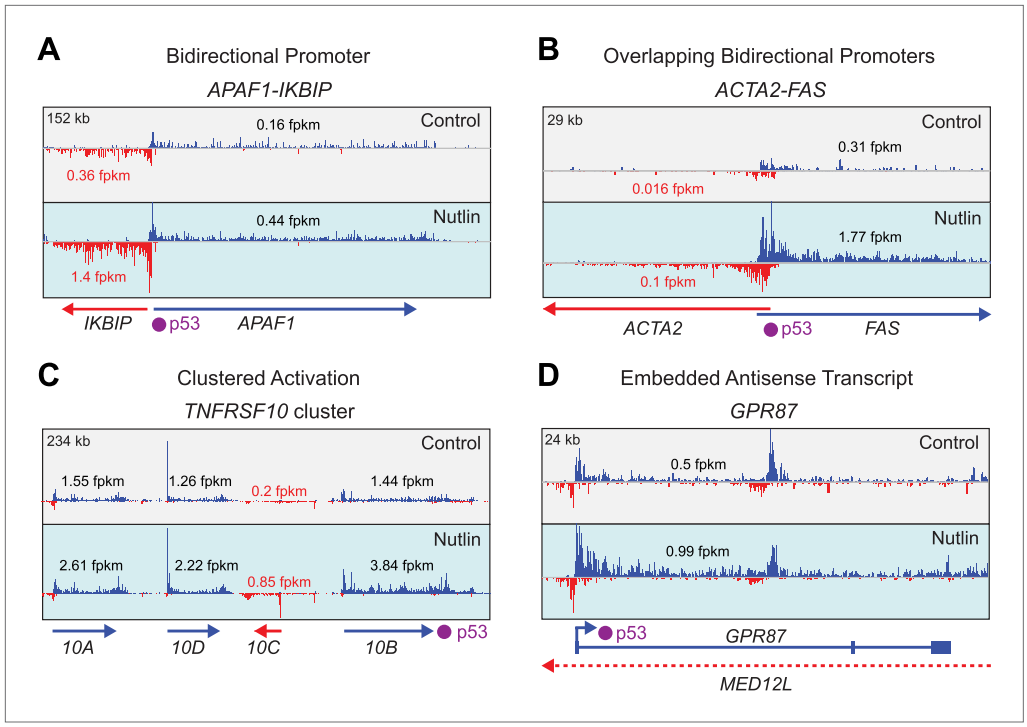

Figure 4—figure supplement 2. Examples of gene-specific features affecting key pro-apoptotic and survival p53 target genes.

DOI: 10.7554/eLife.02200.013

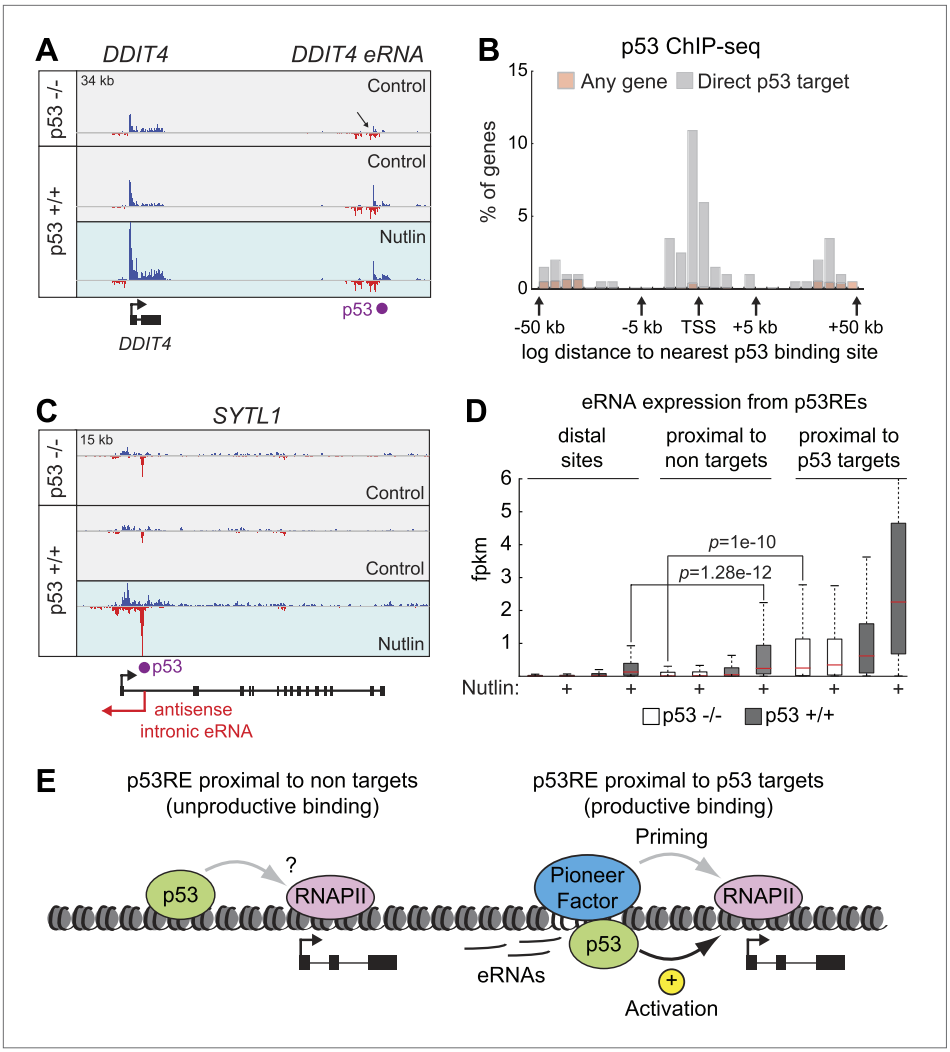

Figure 5. Direct p53 target genes harbor pre-activated enhancers. (**A**) GRO-seq results for the *DDIT4* locus, representative of p53 target genes that display bidirectional eRNA transcription (arrow) arising near sites of p53 binding (indicated by a purple dot). (**B**) Analysis of nearest p53 binding events relative to the transcription start site (TSS) of direct p53 target genes detected by GRO-seq (grey bars) vs all RefSeq genes (pink). (**C**) GRO-seq results for the *SYTL1* locus, representative of p53 target genes that display intronic antisense eRNA transcription arising near sites of p53 binding. (**D**) Analysis of eRNA transcription at distal p53 binding sites (>25 kb of any gene), proximal sites associate with a gene not activated by p53 (<25 kb of non-target), and those proximal to a p53 target gene identified by GRO-seq. (**E**) p53 binding sites near target genes have higher transcription levels than sites near other genes even in p53 null cells, indicating the likely action of pioneer factors.

DOI: 10.7554/eLife.02200.014

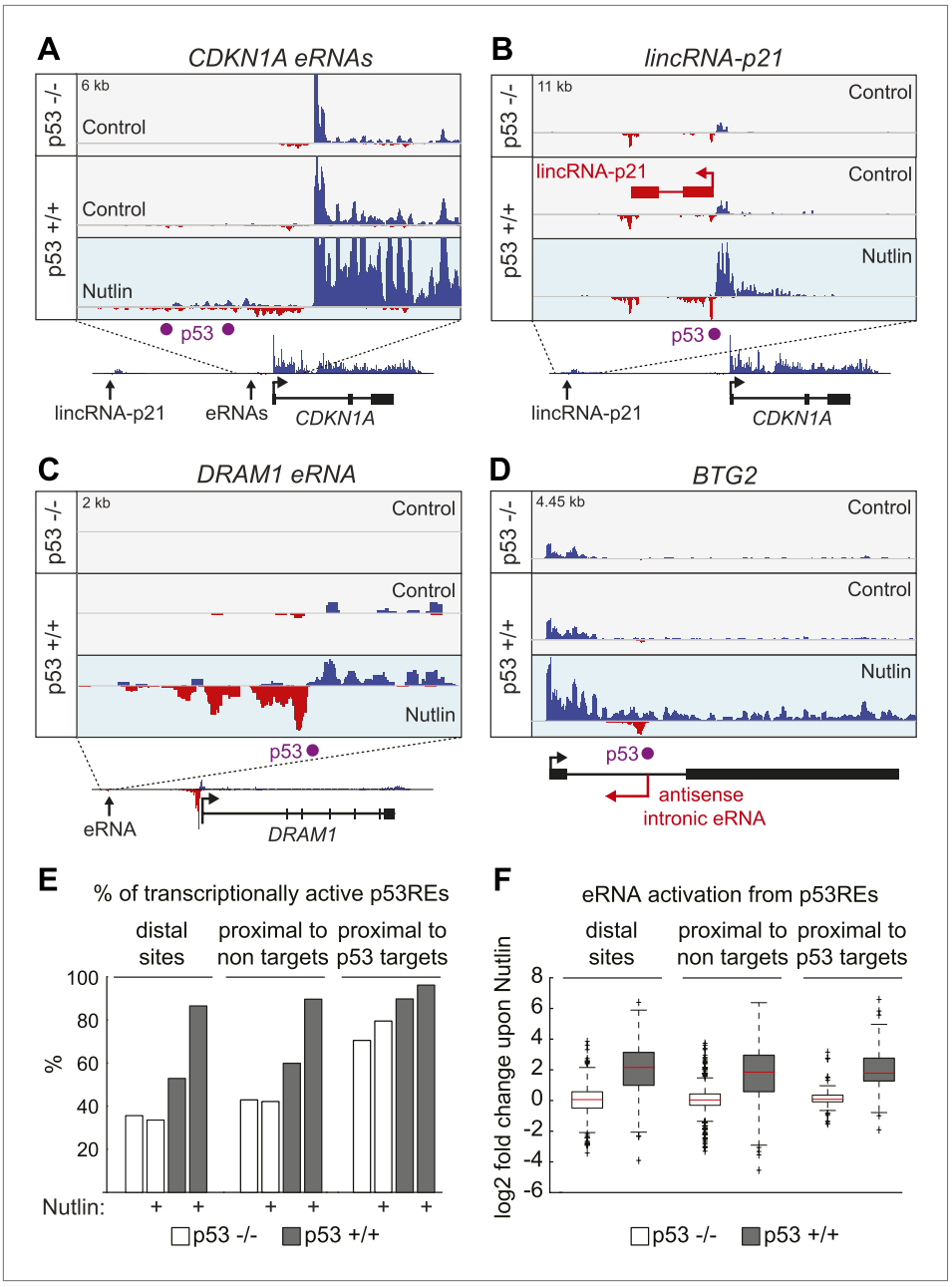

Figure 5—figure supplement 1. p53 stimulates eRNA production at extragenic and intragenic locations.

DOI: 10.7554/eLife.02200.015